JOURNAL OF CATALYSIS 39, 161–172 (1975)

Physicochemical Properties and Structure of $MgMoO_4$–MoO_3 Catalysts

W. OGANOWSKI, J. HANUZA, B. JEZOWSKA-TRZEBIATOWSKA AND J. WRZYSZCZ

Institute of Organic Chemistry, Department of Petrochemistry, Polish Academy of Sciences[1]; *and Institute of Low Temperature and Structure Research, Polish Academy of Sciences, Department of Structural Chemistry,*[2] *Wroclaw, Poland*

Received May 20, 1974; revised March 14, 1975

An attempt was made to elucidate the properties of the $MgMoO_4$–MoO_3 system containing various amounts of MoO_3 which is active in the oxidizing dehydrogenation reaction converting ethylbenzene into styrene. By applying ir, Ra, ESR spectroscopy and the DTA and DTG methods, the samples containing an octahedral phase on the tetrahedral $MgMoO_4$ base were found to have catalytic activity. Besides, the active centers include the Mo(V) ion, most probably in the MoO_5^{5-} type polyhedra with a distorted pyramid structure.

INTRODUCTION

The selective oxidation reactions of hydrocarbons are normally catalyzed by the systems consisting of metal oxides which form either solid solutions, oxy-salt type compounds or mixtures of both. Typical oxidizing dehydrogenation catalysts are, among others, bismuth, cobalt and nickel molybdates. The catalytic properties of the molybdates are related to their structure which depends on the method of preparation and thermal treatment.

Sleight *et al.* (*1*) have shown that Fe(II), Co and Ni molybdates may occur in three structural modifications. The molybdates obtained at high pressures have a wolframite structure while those synthesized under normal pressure at low and high temperatures belong to the space group $C\,2/m$–C_{2h}^3 ($Z = 8$) with a lattice symmetry C_2 and C_s. Their cell dimensions are similar, but they are not isotypic. β-$FeMoO_4$ and β-$NiMoO_4$ are isotypic to α-$MnMoO_4$ and have a tetrahedral structure of the coordination polyhedra. On the other hand α-$FeMoO_4$, α-$NiMoO_4$ and α-$CoMoO_4$ form another group of isotypes with octahedral coordination around Mo.

The structure of magnesium molybdate which is subject to our studies has not been known until now. Abrahams and Reddy (*2*) as well as Young and Schwartz (*3*) suggest that α-$MgMoO_4$ is isotypic with α-$MnMoO_4$.

Structural studies were also carried out on solid solutions consisting of molybdates and molybdenum trioxide, i.e., of the X_2MoO_4–MoO_3 systems where X = K, Rb, Li (*4,5*). X-Ray diffraction studies enabled us to establish the existence of three phases with the following stoichiometric compositions: $X_2Mo_2O_7$, $X_2Mo_3O_{10}$ and $X_2Mo_4O_{13}$ (*4*). The main structural elements of these phases are distorted octahedra in which there occur two short Mo–O bonds (1.67–1.75 Å), two medium bonds in *trans* position to the former one (1.89–2.04 Å) and two long bonds (2.13–2.64).

In the present study an attempt was

[1] W. O., J. W.
[2] J. H., B. J-T.

made to elucidate the properties of the $MgMoO_4$–MoO_3 system which, according to its chemical composition, possessed different activities in the oxidative dehydrogenation of ethylbenzene to styrene. To this effect ir, Ra and ESR spectroscopy as well as DTA methods were used.

EXPERIMENTAL METHODS

I. Preparation of Catalysts

The catalysts were obtained by boiling aqueous suspensions of MgO and MoO_3, MgO and $H_2MoO_4 \cdot 2H_2O$ or $MgCO_3$ and MoO_3. The 10% $MgMoO_4$ solution thus obtained was cooled to room temperature and filtered, then a crystalline precipitate was formed by adding 2 vol of acetone/1 vol of solution. After 24 hr the precipitate was filtered off, washed with acetone and dried for 24 hr at room temperature. Afterwards the catalysts were dried for 4 hr at 120°C and calcined for 2 hr at 550°C, and in one case at 800°C. The active catalysts were prepared either from stoichiometric amounts of reactants or by employing up to about 8% excess MoO_3. On the other hand, inactive catalysts were prepared by introducing 2% excess MgO or $MgCO_3$ as compared with the stoichiometric amounts, into the reaction mixture. The activity of catalysts does not depend on the kind of reactants used for synthesis, but it depends on the amount of excess MoO_3 in the final product. The data pertaining to the catalysts in question are given in Table 1.

II. Characterization of the Catalysts

Catalytic activities were determined in a tubular quartz reactor by the dynamic method without recirculation. Catalyst

TABLE 1
SPECIFICATION OF CATALYSTS EXAMINED

Symbol	Catalyst	Excess MoO_3 and MgO content in $MgMoO_4$ (% by wt)		Calcination temp (°C)	Remarks
		MoO_3	MgO		
a	$MgMoO_4$–MoO_3	—[a]	—	—	Precursor
b	$MgMoO_4$–MgO	—	—	—	Precursor
c	$MgMoO_4$–MoO_3	7.30	—	550	Obtained from precursor a
d	$MgMoO_4$–MgO	—	1.5	550	Obtained from precursor b
e	$MgMoO_4$–MoO_3	7.30	—	550	Cat. c reduced with ethylbenzene at 390°C for 5 hr
f	$MgMoO_4$	0.0	—	800	Cat. c calcined for 6 hr
g	MoO_3	—	—	600	$H_2MoO_4 \cdot 2H_2O$ calcined for 9 hr
h	$MgMoO_4$–MoO_3	0.40	—	550	
i	$MgMoO_4$–MoO_3	1.10	—	550	
j	$MgMoO_4$–MoO_3	1.55	—	550	Catalysts h–s were prepared from precursors containing various excess of MoO_3
k	$MgMoO_4$–MoO_3	2.05	—	550	
l	$MgMoO_4$–MoO_3	3.95	—	550	
m	$MgMoO_4$–MoO_3	4.05	—	550	
n	$MgMoO^4$–MoO_3	4.15	—	550	
o	$MgMoO_4$–MoO_3	4.45	—	550	
p	$MgMoO_4$–MoO_3	5.15	—	550	
r	$MgMoO_4$–MoO_3	6.45	—	550	
s	$MgMoO_4$–MoO_3	8.30	—	550	

[a] — = undetermined.

TABLE 2

INFRARED AND RA SPECTRA OF MgO–MoO_3 CATALYST

$MnMoO_4$		MgO–MoO_3										
		Precursor of active catalyst		Precursor of inactive catalyst		Active catalyst		Inactive catalyst		Active catalyst		
										After usage	Heated up to 800°C	
ir	Ra	ir	Ra	ir	Ra	ir	Ra	ir	Ra	ir	ir	Assignment
3400 w		3400	3650 sb	3400	3650 sb	3358 m		3620 sh 3300 sh 3180 vs		3610 m 3300 vw	—	ν(OH)
1670 w		1675 s,b		1662 m 1681 s		1630 w		1648 m 1634 m		1640 vw 1614 vw	—	δ(HOH)
						985 sh	988 m		990 vw	988 sh	981 vs	ν(Mo=O)
951 sh	948 vs	962 vs	971 w	945 s		962 vs	965 vs	951 vs	966 vs	961 vs	958 sh	$\nu_1(A_1)$ MoO_4^{2-}
941 vs	936 vs		940 vs	920 vs	928 vs	939 vs	955 vs	935 vs	953 vs	934 vs	943 vs,b	
925 s			917 w			921 sh	928 w	925 sh		924 sh	928 sh	$\nu_3(F_2)$ MoO_4^{2-}
915 m	885 m	916 vs	898 w				910 s	900 sh	906 w	900 sh	895 s	
865 s	850 m	862 s	870 s	850 s	840 s	884 vs	877 m	886 vs	875 m	882 vs	880 sh	
792 s,b	830 m	840 vs	845 m	805 s,b		825 s	855 m		851 m			
		783 s				810 sh	814 vw	820 s		816 s	829 s,b	
						766 s		765 s		771 s		
725 s,b			720 vw	730 m		721 m		726 m		729 s	650–770 m,vb	ν(MoOMo)
		623 s,b		550–650 w,vb		660 sh				670 sh	640 sh,vb	
						444 sh	427 vw	439 s		440 sh		$\nu_4(F_2)$ and $\nu_3(MgO_6)MoO_4^{2-}$
403 vs		428 s,b				420 vs	402 vw			414 s		
380 sh			385 w			377 sh	383 m	380 sh	381 m	375 sh		
351 sh	345 m	358 s	365 m			356 vs	372 s	358 s	364 m	352 vs		
344 s												
330 sh			340 sh		345 sh		348 m		345 vs			
302 sh					330 sh		339 s	325 s	330 s			$\nu_2(E)$ MoO_4^{2-} and $\nu_3(MgO_6)$
	301 m		315 s		314 vs	303 s	325 w	310 sh		295 s		
			297 sh			276 sh	276 m		278 m	274 s		
	244 m		245 sh		229 m		250 w		256 vw	241 m		
							227 w		228 vw			$\nu_4(MgO_6)$
			210 m		205 m		204 m		204 vw			
	162 s		165 m				178 w		176 w			
			147 m				156 m		155 w			Rotational and translational modes
	135 w				127 vw		122 w		125 w			
			102 m		95 vw		94 w		95 m			

samples (1 g) ground into 0.2–1.0 mm grains were diluted with quartz of the same grain size in a molar ratio of 1 : 1. Catalytic activities were estimated at 500°C for a contact time of 0.075 g sec/cm^3 at a 1 : 2 molar ratio of ethylbenzene to oxygen. Ethylbenzene was introduced into the reaction zone as a mixture with air. The reaction products were analyzed by gas chromatography methods. The active catalysts yielded 26% styrene and small amounts of benzene, toluene, CO, CO_2 and some solid products. The inactive catalysts yielded under the same conditions about 2% styrene.

Specific surface measurements have shown that it was similar in all cases and amounted to 6–7 m^2/g for samples in which excess percentage of MoO_3 did not exceed 6%.

The ir spectra were measured between 200–4000 cm^{-1} in a Perkin-Elmer 621

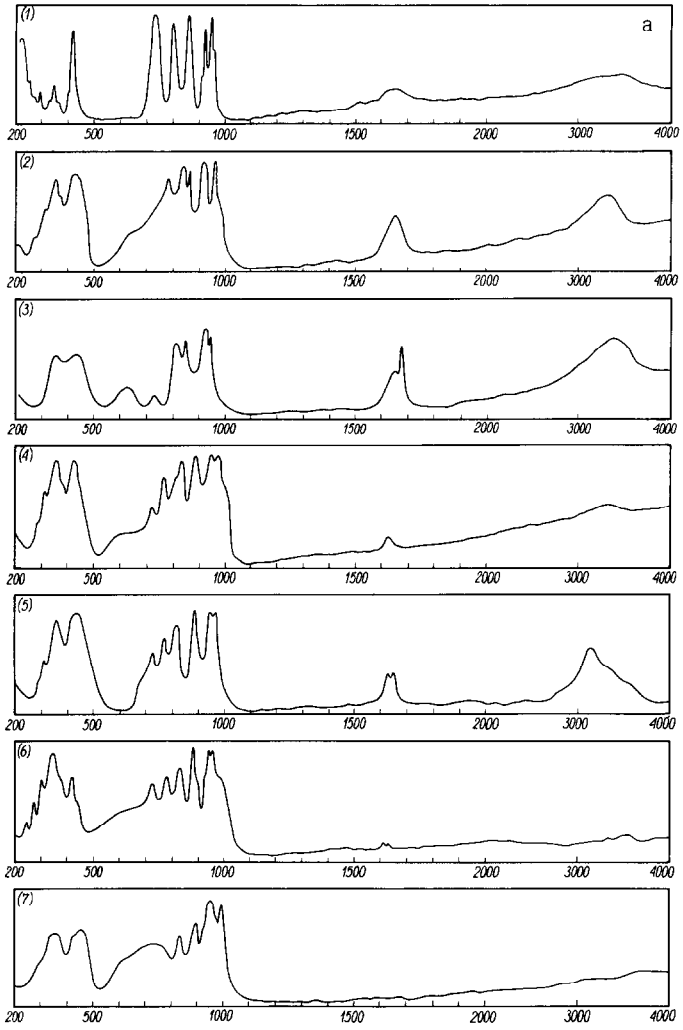

FIG. 1. Infrared and Raman spectra of the Mg/Mo catalyst samples examined: (a) (1) $MnMoO_4$ (ir); (2) precursor of active catalyst (ir); (3) precursor of inactive catalyst (ir); (4) active catalyst (ir); (5) inactive catalyst (ir); (6) active catalyst after usage (ir); (7) active catalyst heated up to 800°C (ir); (b) (8) MoO_3 (ir); (9) $MnMoO_4$ (Ra); (10) precursor of active catalyst (Ra); (11) precursor of inactive catalyst (Ra); (12) active catalyst (Ra); (13) inactive catalyst (Ra).

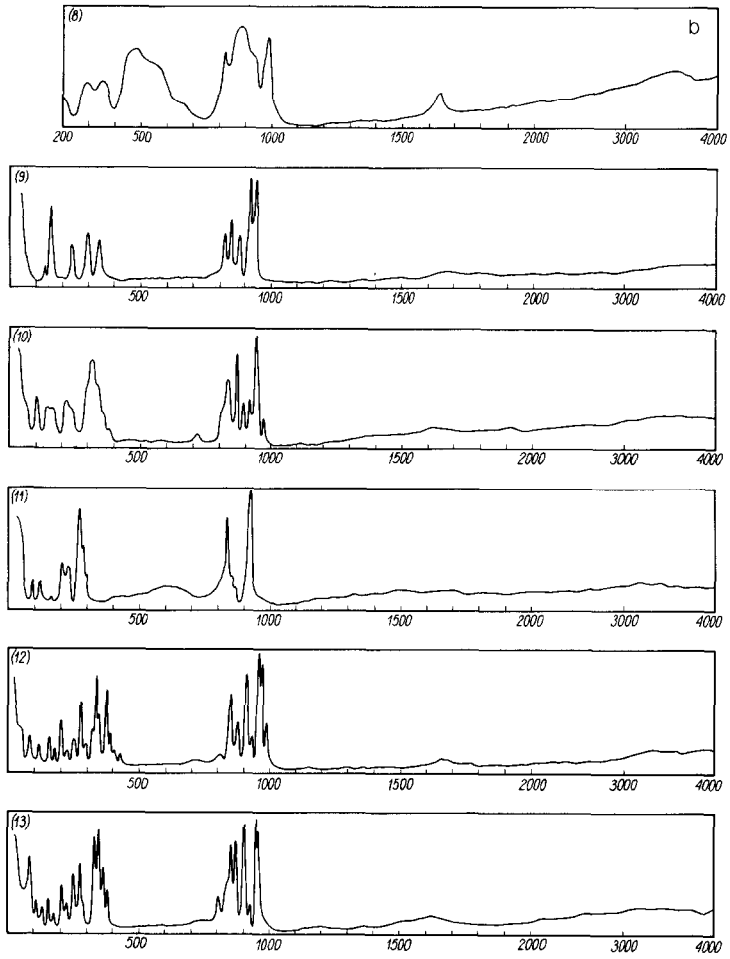

FIGURE 1b.

spectrophotometer by conventional solid state techniques (pressed KBr disc, Nujol and hexachlorobutadiene mulls). The Raman spectra of powders from 50 to 400 cm^{-1} have been recorded in a JEOL Raman spectrophotometer Model 73 equipped with a 200 mW Ar laser. Measurements were carried out by the rotating disc method and in glass capillary tubes.

ESR measurements were made in a JEOL spectrometer Model 3MX at room temperature. Frequencies were determined by means of a free DPPH radical, assuming $G_{DPPH} = 2.0037$.

DTA measurements were made in a MOM derivatograph (F. Paulik, J. Paulik, L. Erdey system) over the temperature range of 20–1000°C.

III. Results and Discussion

A. Infrared and Ra Studies

The ir and Ra frequencies of the samples examined are listed in Table 2 and Fig. 1.

A comparison of the ir and Ra spectra in solid solutions a–f (Fig. 1, Table 2) shows a number of important differences. Some bands possess different contours and differ in their intensities.The intensities and energy sequences of the other bands remain unchanged which indicates that the com-

position of the solutions in question is not uniform. The "constant" band pattern corresponds to magnesium molybdate $MgMoO_4$, high intensities of these bands being an evidence that this component predominates in solid solutions.

Magnesium molybdate is expected to display an isotypic structure with either tetrahedral or octahedral coordination around Mo. A comparison between the spectra of our magnesium molybdates and α-$MnMoO_4$ and that of α-$CoMoO_4$ reported by Cord *et al.* (*6*) shows that the $MgMoO_4$ obtained have a tetrahedral structure of coordination polyhedra which is isotypic to α-$MnMoO_4$. Since magnesium and maganese molybdates have an identical band pattern, one may assume that the basic structural unit of $MgMoO_4$ is the system of tetrahedra in the C_2 and C_s lattice and the space group has a C_{2h}^3symmetry. This is also indicated by the theoretical description of vibrational spectra based upon the group theory (Table 3).

Table 3 presents a correlation of the four frequencies characteristic of the tetrahedron (space group T_d) with the space group symmetry (factor group) C_{2h} and the symmetry in lattice nodes C_2 and C_s. According to this scheme, both in the ir and Ra spectra six groups of bands should be expected to appear in the stretching frequency range $\nu(MoO_4)$ which correspond to the ν_1: $A(C_2)$ and $A'(C_s)$ and ν_3: $A(C_2)$, $B(C_2)$, $A'(C_s)$ and $A''(C_s)$ vibrations, being additionally split as a result of the lattice effect. The main peaks for these frequencies appear (Table 2) in the spectrum of α-$MnMoO_4$ at 941, 925, 915, 865, 792 and 725 cm^{-1} while for the catalysts with a $MgMoO_4$ carrier at 935–968, 910, 880, 820, 770–760 and 730–720 cm^{-1}. It seems therefore, that such a pattern of bands classed in this frequency region is typical of the entire group of tetrahedral molybdates isotypic to α-$MnMoO_4$. A relatively broad stretching vibration energy range of 700–970 cm^{-1} results from a considerably distorted tetrahedron whose Mo–O distances vary from 1.72 to 1.85 Å (*2*). Over the deformation frequency range $\delta(OMoO)$, that is from 450 to 200 cm^{-1}, there is no such a distinct contour as in the case of stretching frequencies. In this range the $\delta(MoO_4)$ and $\nu(MgO_6)$ frequencies overlap, and hence, it is very difficult to assign the bands. In Table 4 we have suggested a description of normal frequencies for the MoO_4^{2-} tetrahedra in lattice nodes C_2 and C_s. Over the energy range below 250 cm^{-1}, the radiation is absorbed by the external modes, that is by the rotational and traslational modes.

It was more difficult to establish the

TABLE 3
CORRELATION DIAGRAMS FOR MoO_4^{2-} VIBRATIONS

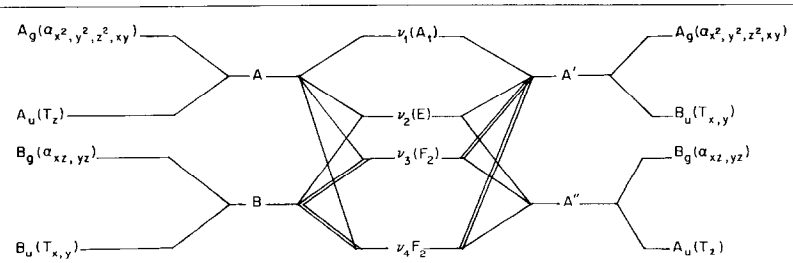

TABLE 4
ASSIGNMENT OF NORMAL MODES OF VIBRATIONS

a[a]	b	c	d	e	C_{2h}	C_2 and C_s	T_d
951	962	945	962	951	A_u (ir)	A (C_2)	ν_1 A_1
948	971		965	966	A_g (Ra)		
941		920	939	935	B_u (ir)	A′ (C_s)	
936	940	928	955	953	A_g (Ra)		
925	916	920	921	925	A_u (ir)	A (C_2)	ν_3 F_2
	917	928	928		A_g (Ra)		
915	916	920		900	B_u (ir)	A′ (C_s)	
885	917	928	910	906	A_g (Ra)		
850	898	840	877	875	A_g (Ra)		
792	783	805	766	765	B_u (ir)		
865	862	850	884	886	A_u (ir)	A″ (C_s)	
	845		814		B_g (Ra)		
	840	805	825	820	B_u (ir)	B (C_2)	
830	870	840	855	851	B_g (Ra)		
725	720	730	721	726	B_u (ir), B_g (Ra)		
403	428	440	444	439	A_u (ir)	A (C_2)	ν_4 F_2
			427		A_g (Ra)		
403	428		420		B_u (ir)	A′ (C_s)	
	385		402	381	A_g (Ra)		
351	358		356	358	B_u (ir)		
	365	345	348	345	A_g (Ra)		
	365		383	364	B_g (Ra)	B (C_2)	
380			377	380	B_u (ir)		
345	365		372		B_g (Ra)		
344	358				B_u (ir)		
330				325	A_u (ir)	A″ (C_s)	
301	340	330	339	330	B_g (Ra)		
302			303	310	A_u (ir)	A (C_2)	ν_2 E
301	315	314	325	330	A_g (Ra)		
300			276		B_u (ir)	A′ (C_s)	
	297		276	278	A_g (Ra)		
280					B_u (ir)	B (C_2)	
244	245	229	227	228	B_g (Ra)		
248					A_u (ir)	A″ (C)	
	210	205	204	204	B_g (Ra)		

[a] a, b–e solid solutions (see Experimental Methods).

structure of another component in solid solutions under investigation. This is because the corresponding bands are rather weak and appear often as shoulders on the slopes of strong and broad $MgMoO_4$ bands. The arrangement of bands as well as their energy levels differ from those of the $MgMoO_4$ spectrum which shows that the molybdenum atom has a different coordination. The nature of the spectra is very similar to that observed for MoO_3 (spectrum 8, Fig. 1) and for α-$CoMoO_4$ (*6*). The ir band positions for MoO_3 and for another component of solid solutions are listed in Table 5.

The structural elements of MoO_3 and α-$CoMoO_4$ are the chains of octahedra in which like in the 2,3 and 4-molybdates discussed above (*4*) three types of interatomic distances Mo–O occur (*7*). Thus the ν(MoO) stretching mode which absorbs in the tetrahedral molybdates over the frequency range of 700–970 cm^{-1}, should appear in the octahedral compounds over a broader region than previously. The ν(MoO) frequency in the spectra of MoO_3 (Table 5) and Fe^{II}, Co and Ni α-molybdates reported by Cord *et al.* (*6*) was, in fact, found to increase up to 980–990 cm^{-1} and, simultaneously, the lower stretching vibration limit to decrease from 700 to 500 cm^{-1}. The former effect results from shorter molybdenum–oxygen bonds in the octahedron. On the other hand, a decrease in frequency below 700 cm^{-1} is indicative of the presence of long bonds [2.30–2.33 Å (*7*)] typical of the octahedral MoO_6^{6-} molecule, apart from the 1.72–2.00 Å bonds characteristic of the MoO_4^{2-} tetrahedra (*2*). The same effects are found in the spectra of solid solutions measured in the present work. The bands

TABLE 5
INFRARED SPECTRUM OF MOLYBDENUM TRIOXIDE AND ACTIVE COMPONENT OF THE CATALYSTS

Active phase frequencies	Pure MoO_3 frequencies	O_h	C_s	V_h^{16} (zx)
985–990	991 s 915 sh	$\nu_1(MoO_6)A_{1g}$	A′	$B_{1u}(T_z)$ $B_{3u}(T_x)$
Obscured	865 s,b 820 s	$\nu_3(MoO_6)F_{1u}$	A′ A″	$B_{1u}(T_z)$ $B_{3u}(T_x)$ $B_{2u}(T_y)$
550–650	660 m,sh 567 s,b 470 s,b	= $\nu_4(MoO_6)F_{1u}$	A′ A″	B_{1u} B_{3u} B_{2u}
Obscured	375 m 300 m	= $\nu_5(MoO_6)F_{2g}$	A′ A″	B_{1u} B_{3u} B_{2u}

corresponding to the second solution component appear at 980 cm^{-1} and over the 550–670 cm^{-1} range. Furthermore, these bands depend directly on the method of catalyst preparation, that is their intensities increase as the MoO_3 contents in solid solution increases. These bands are not found in inactive samples which contain excess MgO ($MgMoO_4$–MgO) or stoichiometric $MgMoO_4$.

In conclusion, it may be stated that the active catalysts form a two-component solid solution $MgMoO_4$–MoO_3 where the $MgMoO_4$ phase has a tetrahedral structure and acts as a "carrier" of the active octahedral phase.

B. DTA and DTG Studies

The DTA and DTG analyses made on the precursors of active and inactive catalysts have shown that no phase transition takes place at temperatures up to 500°C and only a few endothermic and mass effects resulting from loss of water are observed to occur at about 110, 145, 200 and 275°C. It is, however, interesting to note the results of thermodifferential DTA and DTG analyses for active and inactive magnesium molybdates at higher temperatures (Fig. 2).

At temperatures exceeding 600°C an endothermic effect accompanied by the mass decrement is found in both active catalysts and MoO_3. This results most certainly from sublimation of molybdenum trioxide. On the other hand, MoO_3 was not found to sublime in an inactive sample since it does not contain any excess molybdenum trioxide. Pure MoO_3 begins to sublime at a considerably lower temperature than MoO_3 from the active $MgMoO_4$–MoO_3 catalyst. Thus, it may be suggested that in the latter case MoO_3 is more strongly bound to the $MgMoO_4$ "carrier." One may add, however, that with 2 hr heating at 800°C the active catalyst loses its activity due to the loss of excess MoO_3.

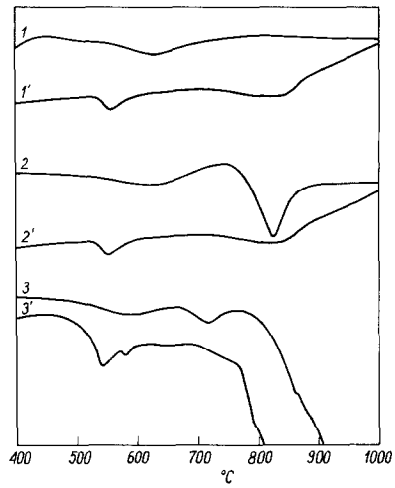

FIG. 2. DTG and DTA analyses of catalysts and MoO_3. Experimental conditions: temp, 20–1000°C; atmosphere in the furnace: air; DTA sensitivity, 1/2; DTG sensitivity, 1/3; heating rate, 10°C/min. (1,1′) active catalyst; (2,2′) inactive catalyst; (3,3′) molybdenum trioxide; (1,2,3) DTG; (1′, 2′, 3′) DTA.

C. ESR Studies

The activity of selective oxidation catalysts is usually related to the formation of a redox-type complex. In our case one could have assumed that it will be related to the formation of a Mo^{5+} ion containing complex. For this reason, ESR spectroscopy methods were applied to the examined catalysts which enabled us to determine the Mo(V) content, to draw certain conclusions on the energy level splitting in the crystal field and enabled us to establish the structures of active centers.

The low Mo(V) concentration in the catalysts, of an order 10^{19} spins/g, was insufficient to apply conventional magnetic methods. Therefore, we have employed ESR spectroscopy. The ESR spectra of all active $MgMoO_4$–MoO_3 catalysts have shown a similar signal which is not found in the samples of MoO_3 and inactive magnesium molybdates. A typical ESR spectrum in the form of an absorption curve and its derivative is presented in Fig. 3.

The spectrum exhibits an asymmetric ESR signal with three factors: $g_x = 1.930$,

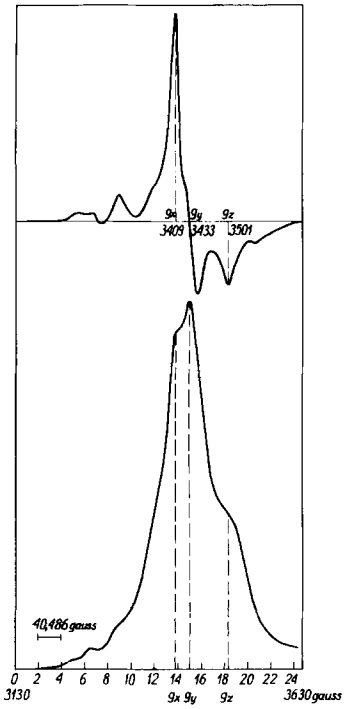

FIG. 3. ESR spectrum of $MgMoO_4$–MoO_3 catalyst.

$g_y = 1.943$ (corresponding to $g_\perp$) and $g_z = 1.893$ of the $g_{||}$ character. The spectrum was calibrated on the basis of the sixth Mn^{2+} line for which $g = 1.886$. The average tensor $\langle g \rangle = 1/3(g_x + g_y + g_z)$ is 1.922 in our case and the line width is about 60 G. This signal is assigned to Mo(V) in an environment of nonaxial symmetry. Only a very weak satelite line absorption, possibly due to the hyperfine structure resulting from the odd isotopes of Mo (^{95}Mo, $J = 5/2$–natural abundance 15.7%; and ^{97}Mo, $J = 5/2$–9.45%) is observed. The spectral curves and signal width remain almost unchanged over the temperature range of 20–500°C. Such a temperature independence of the signal suggests that the main reason of the line broadening is a nonhomogeneous distribution of Mo(V) in the catalyst.

The ESR signal presented in Fig. 3 may be interpreted by means of a spin hamiltonian for the d^1 electron configuration in the field of nonaxial symmetry: $\mathscr{H} = g_xH_xS_x + g_yH_yS_y + g_zH_zS_z$.

As established on the basis of the ir and Ra spectra (Sect. III A), molybdenum trioxide coordinated on a carrier has a distorted octahedral structure. In the first approximation this distortion is described by an axial C_{4v} symmetry and further straining leads to the C_{2v} symmetry. Distortion of the MoO_6^{6-} polyhedron, observed in MoO_3 deposited on a carrier leads to strength decrease of some molybdenum–oxygen bonds. Calcination of the catalysts at high temperatures probably causes the lost of the oxygen atom in the corner of some of distorted octahedrons. Such "oxygen hole" leads to the formation of the penta-coordinated MoO_5^{5-} ion with a C_{2v} orthorhombic pyramidal arrangement.

A correlation of point groups O_h, C_{4v} and C_{2v} with the energy trends maintained is shown in Fig. 4.

The crystal field of the MXY_5 type molecule is then characterized by two parameters Δ and δ while for the C_{2v} molecule by three parameters Δ, δ and η. The $\langle g \rangle$ factor for a paramagnetic molecule with an orbitally nondegenerate ground state differs from 2.0023 due to the mixing of ground and excited states via spin–orbit coupling. The expressions for the $\langle g \rangle$ values for d^1 transition metal oxycations have been introduced by Ballhausen and Gray (*8*):

$$g_z = 2.0023\left(1 - \frac{4\lambda}{\Delta}\right),$$

$$g_x = 2.0023\left(1 - \frac{\lambda}{\eta}\right),$$

$$g_y = 2.0023\left(1 - \frac{\lambda}{\delta}\right),$$

where λ is the spin–orbit coupling constant for the Mo^{5+} ion (in MoO_5^{5+}) contained in the active center of the catalyst. The free ion constant λ is drastically reduced in the

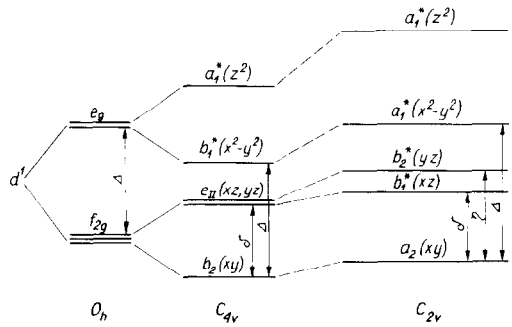

FIG. 4. Energy levels scheme of the Mo(V) ion in a O_h, C_{4v} and C_{2v} fields.

oxycations. For instance, it drops from 380 cm^{-1} for Cr^{3+} to 65 cm^{-1} for $CrOX_5^{2-}$, from 1030 for Mo^{5+} to 240 cm^{-1} for $MoOX_5^{2-}$ and from 2500 for W^{5+} to 500–900 cm^{-1} for WOX_5^{2-} (*9*). Since the λ coupling constant for Mo^{5+} surrounded by the oxygen atoms has not been determined until now, it may only be estimated by analogy with respect to the W^{5+} ions. According to Brisden *et al.* (*9*), for tungsten and molybdenum the λ constant for the MOX_5^{2-} type complexes amounts to 20% of that for the free ion, while for the WOX_4^- complexes—to about 50%. These authors suggest that the WOX_4^- type compounds have higher λ's owing to the interactions between the oxygens of neighboring ions. For our calculations we have assumed the value of 360 cm^{-1} for molybdenum which is 35% of the free Mo^{5+} ion, that is an average value between the MOX_5^{2-} and MOX_4^- oxycompounds. The parameters for such a LS coupling constant of the crystal field calculated from Ballhausen–Gray equation are $\Delta \approx 26{,}200$, $\delta \approx 10{,}000$ and $\eta \approx 12{,}140$ cm^{-1}.

Hence, it may be considered that the active centers of the $MgMO_4$–MoO_3 catalyst contain, apart from the MoO_6^{6-} ions, the Mo(V) ions in polyhedra, most probably of the MoO_5^{5-} type, of a distorted pyramid structure and C_{2v} symmetry. The $\langle g \rangle$ tensor values obtained by us, occurrence of g_x, g_y, g_z anisotropies, as well as the values of crystal field parameters are indicative of rhombic distortion of the molybdenum(V) polyhedra.

Further data were obtained from quantitative measurements of the integral ESR signal intensity of Mo(V) for the above mentioned solid solutions. Quantitative determinations of the spin concentrations were made by the Hyde and Wyard method (*10*), employed also by Seshadri and Petrakis (*11*) in their studies on the Al_2O_3–MoO_3 catalysts. For these calculations a known relationship was used:

$$\frac{N_k}{N_u} = \left(\frac{M_k G_u}{M_u G_k}\right)^{1/2}$$

where N is the number of spins, M = integrated area, G = amplifier gain, k and u = known and unknown sample. A DPPH standard was used for which $N_k = 1.53 \times 10^{21}$ spins/g.

Figure 5a and b show the degree of ethylbenzene conversion in the oxidizing dehydrogenation process and spin concentra-

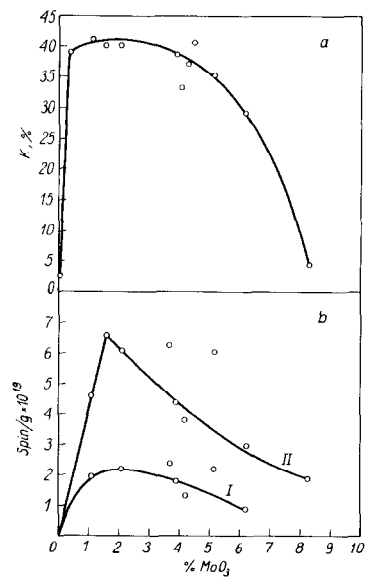

FIG. 5a. Dependence of the K conversion factor for ethylbenzene on excess MoO_3 contents in the catalysts; (b) dependence of spin number on excess MoO_3 contents in catalysts h–s: (I) new, (II) after reduction (reduction with ethylbenzene vapors in N_2 at 390°C for 30 min.

tions in the $MgMoO_4$–MoO_3 samples, fresh and reduced, vs the excess contents of MoO_3. Curve 5a shows that the most active catalysts are those which contain 1–3% of excess molybdenum trioxide. Further increase in the MoO_3 contents result in a decrease of activity. The curves shown in Fig. 5b indicate that the spin concentration in the catalysts varies according to the excess MoO_3 contents like their activity. The Mo(V) contents in the active catalysts varies from 0.9 to 2.4×10^{19} spins/g and increases up to $2.4–6.8 \times 10^{19}$ spins/g on reducing the samples with ethylbenzene vapors. The ratio of spin numbers in the corresponding samples of reduced and new catalysts ranges from about 2 to 3.5. One may note that both the inactive catalysts and samples g (trioxide of molybdenum) were not reduced under these conditions and did not contain any Mo(V).

An increase in the Mo(V) contents in reduced catalysts confirms our above suggestions on the structure of active centers. One may conclude that they are formed from the distorted octahedral MoO_6^{6-} ions linked through an oxygen bridge with the Mo(V) ion in the orthorhombic MoO_5^{5-} pyramidal coordination. These could be one or several Mo(VI) ions per one Mo(V) ion. Such active centers may form a discrete pseudomonomolecular layer coordinated with the tetrahedral support—magnesium molybdate.

REFERENCES

1. Sleight, A. W., *Acta Crystallogr. Sect. B* **28,** 2899 (1972); Sleight, A. W., and Licis, M. S., *Mater. Res. Bull.* **6,** 365 (1971); Sleight, A. W., and Chamberland, B. L., *Inorg. Chem.* **7,** 1672 (1968); Sleight, A. W., and Weiher, J. F., *Inorg. Chem.* **7,** 1093 (1968).
2. Abrahams, S. C., and Reddy, J. M., *J. Chem. Phys.* **43,** 2533 (1965).
3. Young, A. P., and Schwartz, C. M., *Science* **141,** 348 (1963).
4. Gatehouse, B. M., and Miskin, B. K., *J. Solid State Chem.* **9,** 247 (1974); Gatehouse, B. M., and Leverett, P., *J. Chem. Soc. A* 2107 (1971); *J. Chem. Soc. A* 1398 (1968); *J. Chem. Soc. A* 849 (1969).
5. Magarill, S. A., and Klevtsova, R. F., *Sov. Phys. Crystallogr.* **16,** 645 (1972).
6. Cord, P. P., Courtine, P., Pannetier, G., and Guillermett, J., *Spectrochim. Acta Part A* **28,** 1601 (1972).
7. Smith, G. W., and Ibers, J. A., *Acta Crystallogr.* **19,** 269 (1965).
8. Ballhausen, C. J., and Gray, H. B., *Inorg. Chem.* **1,** 111 (1962).
9. Brisden, B. J., Edwards, D. A., Machin, D. J., Murray, K. S., and Walton, R. A., *J. Chem. Soc. A* 1825 (1967).
10. Alger, R. S., "Electron Paramagnetic Resonance: Techniques and Applications," pp. 212–220. Wiley (Interscience), New York, 1968.
11. Seshardri, K. S., and Petrakis, L., *J. Phys. Chem.* **74,** 4102 (1970).